

---

EFDA–JET–CP(04)03-36

P. Mantica, F. Imbeaux, M. Mantsinen, D. Van Eester, A. Marinoni, N. Hawkes,  
E. Joffrin, V.Kiptily, S. Pinches, A.Salmi, S. Sharapov, I. Voitsekhovits,  
P. de Vries, K.-D. Zastrow and JET EFDA Contributors

# Power Modulation Experiments in JET ITB Plasmas



# Power Modulation Experiments in JET ITB Plasmas

P. Mantica<sup>1</sup>, F. Imbeaux<sup>2</sup>, M. Mantsinen<sup>3</sup>, D. Van Eester<sup>4</sup>, A. Marinoni<sup>5</sup>, N. Hawkes<sup>6</sup>,  
E. Joffrin<sup>2</sup>, V.Kiptily<sup>6</sup>, S. Pinches<sup>7</sup>, A.Salmi<sup>3</sup>, S. Sharapov<sup>6</sup>, I. Voitsekhovits<sup>6</sup>,  
P. de Vries<sup>8</sup>, K.-D. Zastrow<sup>6</sup> and JET EFDA Contributors\*

<sup>1</sup>*Istituto di Fisica del Plasma, EURATOM-ENEA-CNR Association, Milan, Italy*

<sup>2</sup>*Association Euratom-CEA, CEA Cadarache, St Paul-lez-Durance Cedex, France*

<sup>3</sup>*Helsinki Univ. of Technology, Association Euratom-Tekes, P.O.Box 2200, Finland*

<sup>4</sup>*LPP-ERM/KMS, Association Euratom-Belgian State, TEC, B-1000 Brussels, Belgium*

<sup>5</sup>*Politecnico di Milano, Dipartimento di Ingegneria Nucleare, Milano, Italy*

<sup>6</sup>*EURATOM/UKAEA Fusion Association, Culham Science Centre, Abingdon, Oxon, OX14 3DB, UK*

<sup>7</sup>*Max-Planck-Institut für Plasmaphysik, EURATOM Association, Garching, Germany*

<sup>8</sup>*FOM-Instituut voor Plasmafysica, Assoc. Euratom-FOM, Nieuwegein, The Netherlands*

\* See annex of J. Pamela et al, "Overview of Recent JET Results and Future Perspectives",  
*Fusion Energy 2002 (Proc. 19<sup>th</sup> IAEA Fusion Energy Conference, Lyon (2002)).*

Preprint of Paper to be submitted for publication in Proceedings of the  
31st EPS Conference,  
(London, UK. 28th June - 2nd July 2004)

“This document is intended for publication in the open literature. It is made available on the understanding that it may not be further circulated and extracts or references may not be published prior to publication of the original when applicable, or without the consent of the Publications Officer, EFDA, Culham Science Centre, Abingdon, Oxon, OX14 3DB, UK.”

“Enquiries about Copyright and reproduction should be addressed to the Publications Officer, EFDA, Culham Science Centre, Abingdon, Oxon, OX14 3DB, UK.”

## ABSTRACT

Power modulation experiments are a well known tool to investigate electron heat transport and have been widely used in conventional L-mode or H-mode plasmas. In this paper new results are presented of power modulation experiments in JET plasmas characterized by strong electron and ion Internal Transport Barriers (ITB).

The modulated power source is RF ICRH power in mode conversion scheme, which takes place in D plasmas with  $^3\text{He}$  concentrations of 10-20% [1, 2]. This provides a source of direct, localized and controllable power to electrons, suitable for transport studies of electron ITBs. The ECE diagnostic allows time and space resolved measurements of the  $T_e$  perturbation. 3.25-3.6T, 2.6-2.9MA plasmas with  $n_{e0} \sim 3\text{-}5 \cdot 10^{19} \text{ m}^{-3}$  have been used. LH preheat (2-3MW) was applied to achieve configurations with deeply reversed magnetic shear ( $s$ ). The ITB is located in the region of negative  $s$ . Up to 18MW of NBI power and 4MW of ICRH power modulated with half depth at 15-45Hz with duty cycle  $\sim 60\%$  were applied. The MC power has been localized either at the ITB layer, providing a heat wave generated in the ITB region, or just outside it, providing a heat wave that travels towards the ITB. The ITB is mainly sustained by NBI power, but when the RF is deposited inside the ITB radius, the good localization of power allows to reach outstanding plasma performance, with  $T_{i0} \sim 24\text{keV}$ ,  $T_{e0} \sim 13\text{keV}$ ,  $n_{e0} \sim 5 \cdot 10^{19} \text{ m}^{-3}$ , at an additional total power level of 15MW. The equivalent  $Q_{DT}$  is estimated to be  $\sim 0.25$  in these discharges.

## 1. EXPERIMENTAL RESULTS

Two RF deposition schemes have been explored: a)  $^3\text{He}$  concentration  $\sim 12\%$  (mixed minority heating and mode conversion), which led to the best ITB performance; b)  $^3\text{He}$  concentration  $\sim 20\%$  (full mode conversion regime), which allowed the best transport studies. Figures 1 and 2 show steady-state profiles of  $T_e$ ,  $T_i$ ,  $n_e$ ,  $q$  and profiles of amplitudes ( $A$ ) and phases ( $\phi$ ) at 1 st harmonic of the  $T_e$  heat wave obtained by standard FFT techniques. Figure 1 refers to one case of type a) in which the MC power was located in the ITB layer; the heat wave is then travelling in two directions away from the ITB. Figure 2 refers to a case of type b) in which the MC was located just outside the (weaker) ITB. Note that in this case a fraction of the power is also deposited to electrons in the centre via fast wave Landau damping, so there are two heat waves propagating towards the ITB, one from the centre and one from the outer region.

Maximum care needs to be taken when performing the FFT analysis of  $T_e$  modulation data to derive profiles of  $A$  and  $\phi$ . In fact an intense MHD activity is often present in these plasmas, with frequent crashes due to internal kink modes (typically  $m=2$ ,  $n=1$ ). These crashes if included in the analyzed time interval generate a broad low frequency spectrum (0-25Hz) which is peaked in space at the ITB radius and pollutes the real heat wave signal.

Only data exhibiting in the  $T_e$  frequency spectrum a clear peak at the modulation frequency well above the continuum background have been retained in this paper and for the modelling work. Figure 2 is particularly interesting because it shows that the heat wave is strongly damped when meeting the ITB from either side, implying that ITBs are narrow layers of very low heat diffusivity

( $\chi_e$ ). In addition, it shows that  $\chi_e$  is not uniform inside the ITB: looking at the slopes of A and  $\phi$ , one can see that the inner part has lower  $\chi_e$ , i.e. a stronger stabilization of turbulence. The outer part shows reduced  $\chi_e$  compared to outside ITB, but still higher than in the inner ITB region. This could correspond to partial stabilization. This observation is in agreement with earlier perturbative studies of JET ITBs using cold pulses from the edge [3]. The cold pulse showed a growth when meeting the ITB foot (corresponding to transport re-enhanced in the more fragile outer ITB part) and then a strong damping further inside. The latter result was also reproduced by turbulence simulations [4]. On the other hand, no sign of amplification of the heat wave when it meets the ITB foot is observed, consistent with the picture of an erosion of the ITB by cold pulses due to increased temperature gradient associated with the cold wave.

## 2. MODELLING MODULATION DATA

Attempts to model these experimental results are in progress. Unlike the case of cold pulses, unfortunately turbulence simulations are not feasible for a modulation experiment at 15-45 Hz due to the long time intervals that it would be necessary to cover. The situation of first principle 1D models like the Weiland [5] and GLF23 [6] models is not satisfactory at all. In fact the Weiland model does not contain the  $s < 0$  stabilization mechanism that seems to play a crucial role in JET reverse shear ITBs [7]. On the other hand, also attempts to model the results using GLF23 did not succeed in reproducing the ITB location and strength in first place, so no meaningful comparison with the modulation results was possible.

Empirical models have therefore mainly been used. Basically two types of empirical models were employed: either a simple constant  $\chi_e$  profile with a ‘‘hole’’ at the ITB location as illustrated in Fig.3(a) and 4(a), or the critical gradient model presented in [4, 8], featuring an increase of turbulent transport above a critical value of the inverse temperature gradient length  $R/L_{Te}$ :

$$\chi_e = \chi_s q^{1.5} \frac{T_e}{eB} \frac{\rho_s}{R} \frac{-R\partial_r T_e}{T_e} - \kappa_c \left( H \frac{-R\partial_r T_e}{T_e} - \kappa_c \right) + \chi_0 q^{1.5} \frac{T_e}{eB} \frac{\rho_s}{R} \quad (1)$$

where  $\rho_s = \sqrt{m_i T_e / eB}$ ,  $q$  is the safety factor,  $\chi_0$  and  $\chi_s$  are dimensionless numbers giving respectively the residual and turbulent transport assuming a gyro-Bohm normalization,  $\kappa_c$  is the threshold, which was assumed higher in the ITB layer than in the rest of the plasma in order to suppress the turbulent contribution to  $\chi_e$ . Figures 3 and 4 illustrate the results of the simulations of Pulse No's: 59397 and 62077 using the simple constant  $\chi_e$  model.

In the case of deposition at the ITB (Fig.3), provided a rather narrow deposition profile is used for the MC deposition, the agreement with  $T_e$  and A is reasonably good at all harmonics, but the modelled phases are significantly lower than the experimental one. Modelling with the empirical gradient model of Eq.(1) did not yield significant improvement in the reproduction of data. Other possible spurious effects besides MHD crashes effects have been explored. Modulation of the Shafranov shift was shown to affect the amplitude peak by 10-15eV at most. Modulation of the location of the ITB boundaries or of the depth of the  $\chi_e$  reduction were shown not to play an important role as they would generate features

that are not seen in the data. However, modelling modulation data of shots of similar type but with higher modulation frequency generally results in better agreement also with phase profiles, suggesting the discrepancy with the simulation at lower frequencies may come from some low frequency non-diffusive contribution to the heat wave propagation, including still the possibility of remaining MHD activity contamination, which may be particularly nasty in these cases where the RF power is deposited in the ITB layer.

Matching the phase values does not instead seem a problem in the case of propagation towards the ITB (Fig.4). Of course the simple model used in Fig.4 is not able to fully account for the physics involved, in particular the variation of  $c_e$  within the ITB which is also required to match the  $T_e$  profile shape and which may result from a threshold profile increasing towards the inner ITB part due to magnetic shear becoming progressively more negative. However even this simple model is capable of reproducing the gross experimental evidence. We expect that a finer reproduction of the experimental features will come from simulations that are in progress using the critical gradient model with a properly shaped threshold profile.

## CONCLUSIONS

For the first time  $T_e$  modulation experiments in plasmas characterized by strong ion and electron ITBs in configurations with reversed  $q$  profile have been performed. Modulated RF power was located either at the ITB location or just outside it. The ITB behaves as a narrow layer of reduced heat diffusivity which stops rapidly the heat wave propagation. The ITB inner part appears characterized by best stabilized turbulence and lower  $c_e$ . The outer ITB part has higher  $c_e$  and is more fragile. Modelling these results with either empirical or first principle transport models is in progress and preliminary results have been presented.

## ACKNOWLEDGEMENT

We thank X.Garbet, A.Thyagaraja, C.Angioni and F.Meo for precious discussions. This work has been conducted under the European Fusion Development Agreement.

## REFERENCES

- [1]. M.Mantsinen et al., Nuclear Fusion **44** (2004) 33.
- [2]. D.Van Eester et al., proc. 15th Top. Conf. on RF Power in Plasmas, May 2003, Wyoming, USA.
- [3]. P.Mantica et al., Plasma Phys. Control. Fusion **44** (2002) 2185–2215.
- [4]. P.Mantica et al., in Proc. 30th Eur. Conf. St.Petersburg, 2003, O-3.1A, European Physical Society ECA Vol.27A (2003).
- [5]. J. Weiland, "Collective modes in inhomogeneous plasma", Kinetic and Advanced Fluid Theory, IoP Publishing, Bristol and Philadelphia 2000.
- [6]. R.E.Waltz et al., Phys.Plasmas **4** (1997) 2482.
- [7]. X. Garbet et al., Nucl. Fusion **43** (2003) 975–981.
- [8]. X.Garbet et al., "Profile stiffness and global confinement", accepted for publication in Plasma Phys. Control. Fusion.

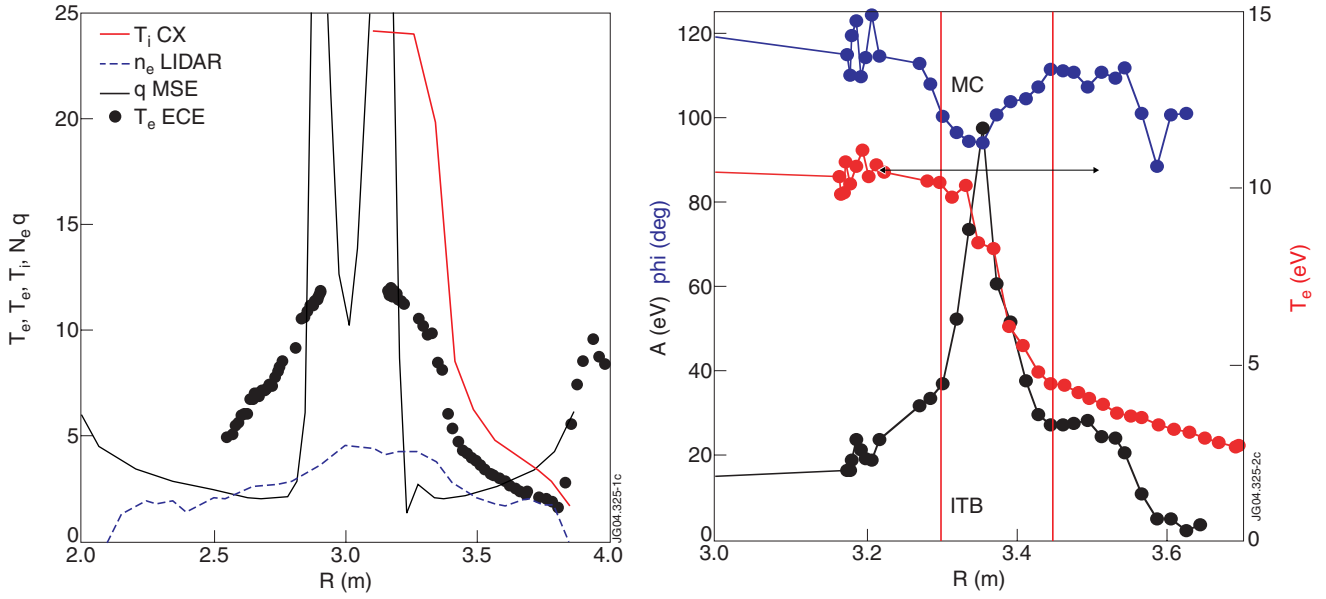


Figure 1: (a) Experimental profiles at  $t = 8$  s (maximum performance) of electron and ion temperatures, density and safety factor for Pulse No: 59397 (3.45T/2.8MA,  $^3\text{He}$  concentration  $\sim 12\%$ , ICRH  $f = 33\text{MHz}$ ). (b) profiles of  $T_e$  (red), amplitude (black) and phase (blue) at 1st harmonic of the modulation frequency (15Hz) during the time interval 6.2-6.48 s. Mode converted modulated RF power is applied at the ITB location.

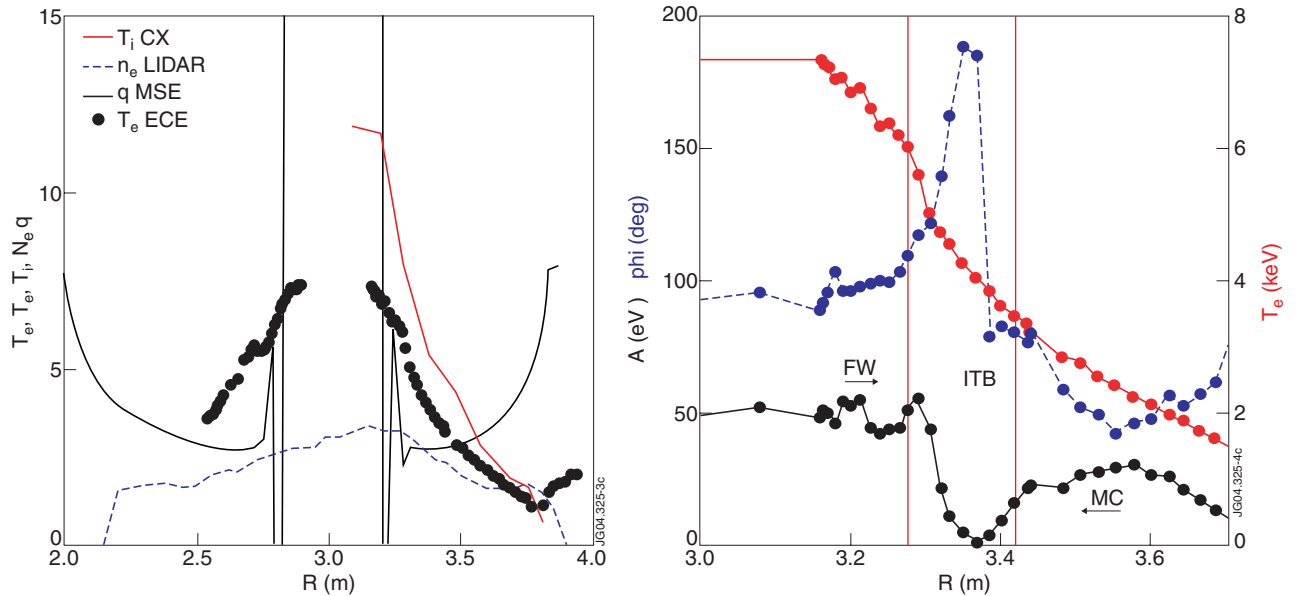


Figure 2: (a) Experimental profiles at  $t = 5.5$  s of electron and ion temperatures, density and safety factor for Pulse No: 62077 (3.25T/2.6MA,  $^3\text{He}$  concentration  $\sim 20\%$ , ICRH  $f = 37\text{MHz}$ ). (b) profiles of  $T_e$  (red), amplitude (black) and phase (blue) at 1st harmonic of the modulation frequency (20Hz) during the time interval 5.5-5.7s. Mode converted modulated RF power is applied outside the ITB location.



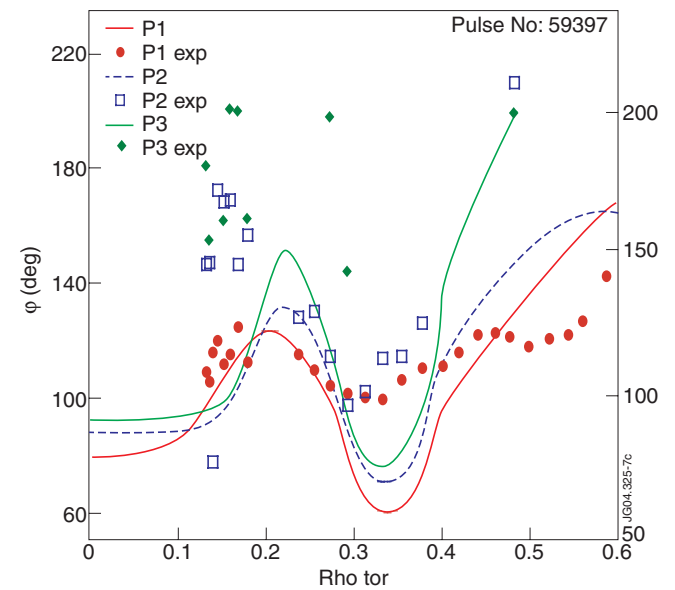
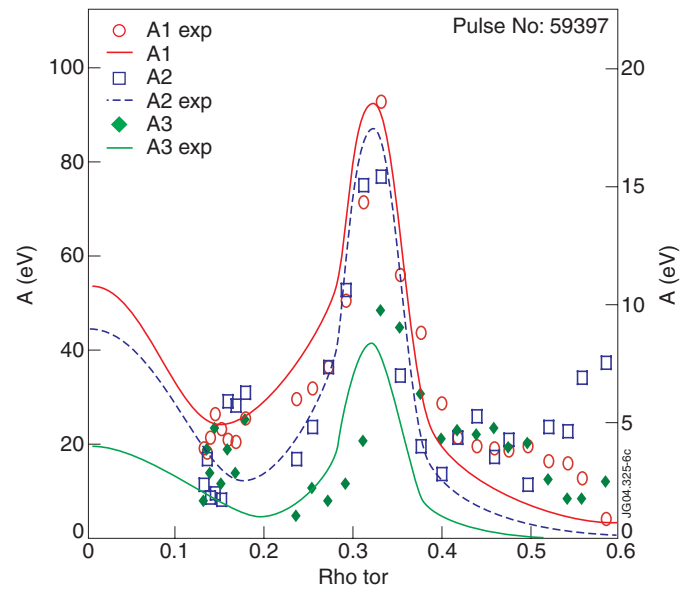
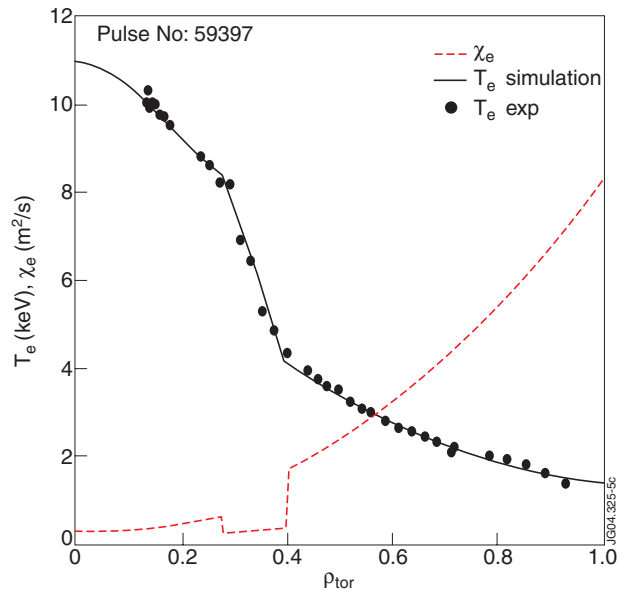


Figure 3: Experimental (dots) and simulated (lines) profiles of (a)  $T_e$ , (b) amplitudes and (c) phases at 3 harmonic for Pulse No: 59397. In (a) also the (constant)  $\chi_e$  profile used in the simulation is plotted.

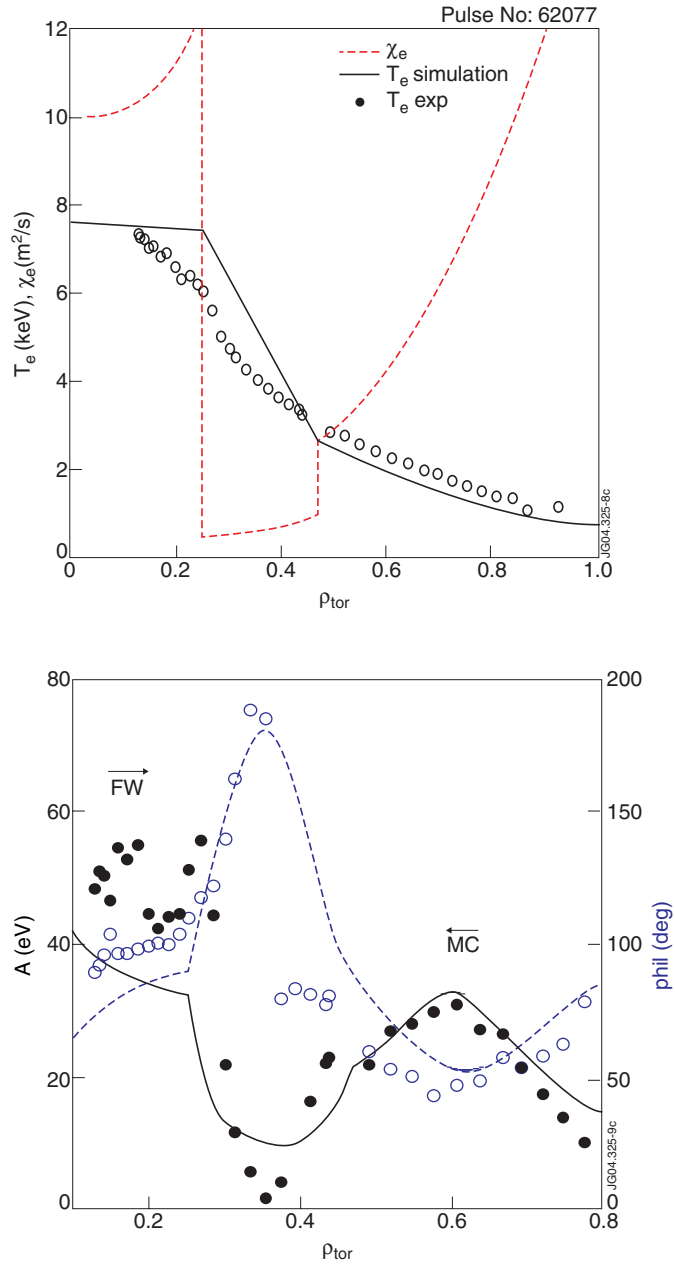


Figure 4: Experimental (dots) and simulated (lines) profiles of (a)  $T_e$ , (b) amplitudes and (c) phases at 1st harmonic for Pulse No: 62077. In (a) also the (constant)  $\chi_e$  profile used in the simulation is plotted.